Journal of Energy Storage 55 (2022) 105584

Contents lists available at ScienceDirect

Journal of Energy Storage

journal homepage: www.elsevier.com/locate/est

Supercooled sodium acetate aqueous solution for long-term heat storage to support heating decarbonisation

Jesus Lizana [a,b,*], Pedro E. Sanchez-Jimenez [b,c], Ricardo Chacartegui [d], Jose A. Becerra [d], Luis A. Perez-Maqueda [b,**]

[a] Department of Engineering Science, University of Oxford, Parks Road, Oxford OX1 3PJ, United Kingdom
[b] Instituto de Ciencia de Materiales de Sevilla, Consejo Superior de Investigaciones Científicas, Universidad de Sevilla, Calle Américo Vespucio 49, 41092 Seville, Spain
[c] Departamento de Química Inorgánica, Facultad de Química, Universidad de Sevilla, Calle Profesor García González 1, 41012 Seville, Spain
[d] Departamento de Ingeniería Energética, Universidad de Sevilla, Camino de los Descubrimientos s/n, 41092 Seville, Spain

ARTICLE INFO

Keywords:
Thermal energy storage
Phase change material
Sodium acetate
Supercooled liquid
Stable supercooling
Heat battery

ABSTRACT

Heating decarbonisation through electrification requires the development of novel heat batteries. They should be suitable for the specific application and match the operation conditions of domestic renewable energy sources. Supercooled liquids, often considered a drawback of phase change materials, are among the most promising technologies supporting heating decarbonisation. Although some studies have shed light on stable supercooling, the fundamentals and stability remain open problems not always accompanied by relevant experimental investigations. This research critically analyses the physic and chemistry of sodium acetate *(SA, $NaCH_3COO$)* aqueous solution, a low-cost, non-toxic, and abundant compound with stable supercooling for long-term heat storage. It has an appropriate phase change temperature for high-density heat storage using heat pumps or solar thermal technologies in residential applications. The existing discrepancies in literature are critically discussed through a systematic experimental evaluation, providing novel insights into efficient material design and appropriate boundary conditions for reliable material use in long-term heat batteries. Despite previous studies showing that the thermal reliability and stability of sodium acetate aqueous solution as a supercooled liquid for heat storage cannot be guaranteed, this study demonstrates that through an appropriate encapsulation and sealing method, the peritectic composition of sodium acetate solution (p-SA 58 wt%) can be used as a supercooled liquid for long-term heat storage with a stable melting temperature of 57 °C, appropriate for domestic heat technologies. It is demonstrated that energy storage efficiency can be maintained under cycling, with a constant latent heat storage capacity of 245 kJ/kg and a volumetric storage density of 314 MJ/m^3. It was confirmed that the material should achieve a fully-melted state for stable supercooling. Finally, local cooling and retaining seed crystals through high pressure were highlighted as the most suitable basic principles for successful crystallization and heat release. This promising material can store energy for long periods without latent heat losses due to its stable subcooling. Latent heat can be released when required at any selected time and temperature just by a simple activation process.

1. Introduction

Reducing greenhouse gas emissions from buildings requires the complete decarbonisation of the heating sector [1,2], responsible for approximately 40 % of final energy consumption, where 75 % is still based on fossil fuels [3]. The decarbonisation of heat through electrification is highlighted as the most promising alternative [4]. However, it could cause a significant increase in peak power demand, adversely affecting the electricity system, above all in highly gas-dependent regions [4,5].

The opportunity for flexible electricity systems based on renewable energy sources and heat storage in buildings is moving rapidly through global energy policy discourse [6]. Recent studies show that heating flexibility solutions in buildings can efficiently shift heat consumption to off-peak hours by up to 29 %, achieving economic savings of 20 % for end-users and reducing the associated electricity cost due to cheaper low-carbon energy generation technologies [7]. Heitkoetter et al. [8]

* Correspondence to: J. Lizana, Department of Engineering Science, University of Oxford, Parks Road, Oxford OX1 3PJ, United Kingdom.
** Corresponding author.
E-mail addresses: jesus.lizana@eng.ox.ac.uk (J. Lizana), maqueda@icmse.csic.es (L.A. Perez-Maqueda).

https://doi.org/10.1016/j.est.2022.105584
Received 23 November 2021; Received in revised form 9 August 2022; Accepted 27 August 2022
Available online 16 September 2022

Nomenclature

DSC	differential scanning calorimetry
$NaCH_3COO$	sodium acetate
PCM	phase change material
p-SA	peritectic sodium acetate aqueous solution
PTFE	polytetrafluoroethylene
SA	sodium acetate
SAT	sodium acetate trihydrate
SD	standard deviation
T	temperature, °C
TES	thermal energy storage
TGA	thermogravimetric analysis

Greek letters

ΔT	temperature difference, °C
ΔH	latent heat of fusion per unit mass, kJ/kg

Subscript and superscript

amb	ambient

reported that energy investment costs could be reduced by 23 % through efficient load shifting by heat pump flexibilization. Interactive real-time pricing has been demonstrated to effectively reduce peak loads and increase the off-peak load, thereby stabilizing the load fluctuation [9]. However, this integration still requires more efficient, reliable, high-density and long-term thermal energy storage (TES) systems to increase the load shifting capacity [10].

Heat storage to support energy flexibility should also be suitable for the desired application and match the operation condition of efficient electric heat pumps and other renewable heat technologies in buildings [11]. In this case, the thermal storage temperature range is crucial. Storage temperature should be adapted according to space heating, and hot water needs since higher flow temperature in the storage mode can reduce the unit's efficiency [12]. Thus, it is recommended that storage temperature ranges between 40 and 60 °C according to the operating temperature of common domestic heat technologies [13].

Many TES compounds have been proposed to increase the share of renewable energy in the heating sector. Among them, heat storage in the form of latent heat has attracted much attention since phase change materials (PCM) can store a more significant amount of heat in a short temperature range when the material undergoes a phase change from a physical state to another [14,15].

Fig. 1 illustrates the most common experimentally tested PCMs (Fig. 1a) [16] and commercially developed PCMs (Fig. 1b) [14]. Each dot represents a PCM according to the melting temperature (°C) on the x-axis and volumetric latent heat storage capacity (MJ/m^3) on the y-axis. Sensible TES processes in water for heating and cooling applications are also illustrated as a reference value (dashed yellow line). This figure allows identifying the PCMs with the highest volumetric storage capacity and with an appropriate melting temperature for thermal applications: below 21 °C for cooling applications, between 22 °C and 28 °C for comfort solutions, and over 30 °C for hot water, space heating, and solar applications.

Experimentally tested PCMs in Fig. 1a include organic compounds (paraffins, fatty acids, esters, sugar alcohols, polyethylene glycols and others), inorganic materials (salt hydrates and metals) and eutectic mixtures (mixtures of inorganics and/or organics). Salt hydrates, characterized by the general formula: salt·xH_2O, are identified as the best available compounds with storage densities up to 514 MJ/m^3 [17]. They are non-flammable and low-cost and present high thermal conductivity compared to organic compounds [18,19]. However, they often show some disadvantages which limit their applicability, such as phase segregation and subcooling, which reduce thermal stability and reliability [20,21], corrosiveness [16] and high thermal expansion during the phase change [22]. Phase segregation refers to converting a single-phase system into a multi-phase system, and supercooling is related to a liquid existing at a temperature lower than the melting temperature.

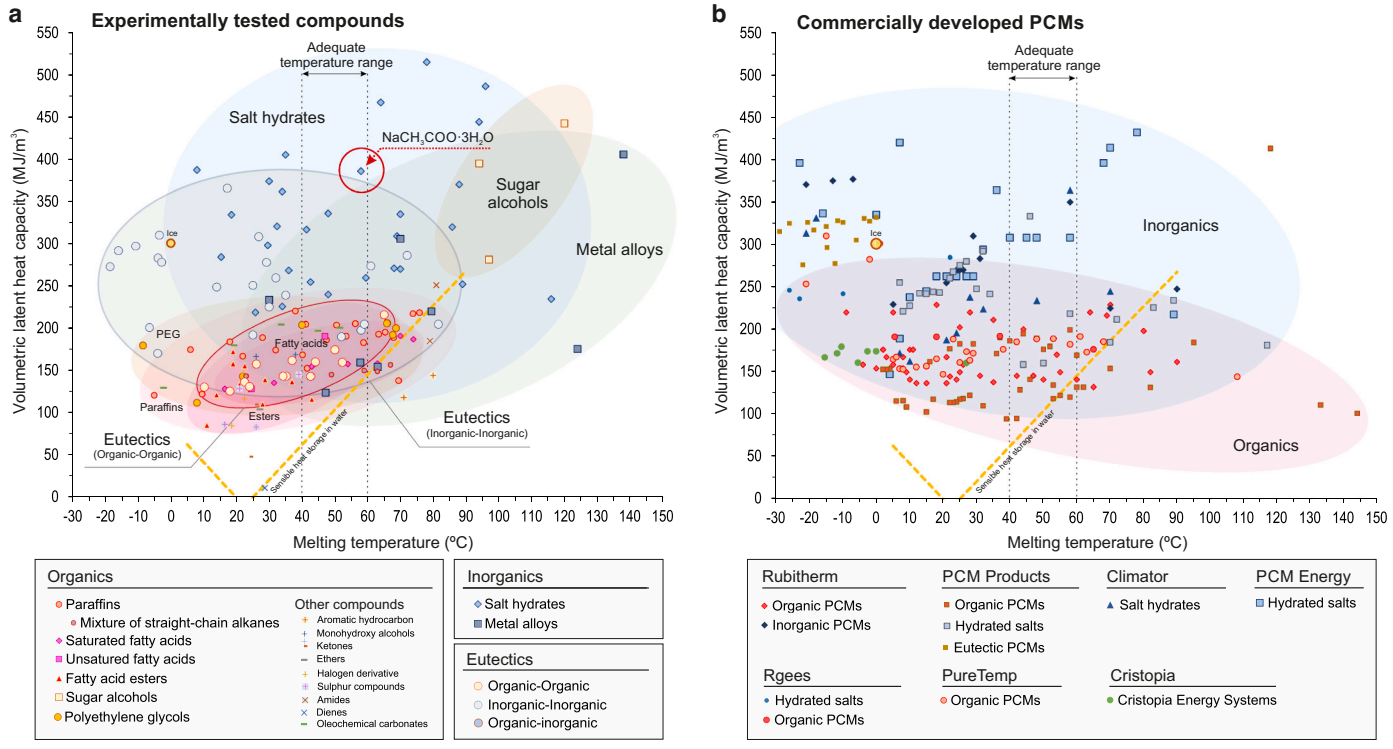

Fig. 1. Overview of phase change materials. a, Experimentally tested latent heat storage compounds and selected material for long-term thermal energy storage (SAT, $NaCH_3COO·3H_2O$). b, Commercially developed PCMs.

In the temperature range for hot water and space heating applications (vertical dashed black lines in Fig. 1a and b between 40 and 60 °C), sodium acetate trihydrate (SAT, $NaCH_3COO{\cdot}3H_2O$) is highlighted as one of the most promising heat storage compounds (highlighted with a red circle in Fig. 1a). Its benefits lie in its high thermal storage density (514 MJ/m^3), a phase change temperature at 58 °C appropriate for domestic heating applications (40–60 °C), low cost, non-toxicity and abundance [16,19]. Moreover, in comparison with thermochemical storage, SAT, along with other PCMs, has the advantage of not requiring auxiliary components, such as tanks and heat exchangers, which significantly reduce the final energy density of thermochemical storage by more than 50 % [14,23]. However, the main drawbacks of SAT, similar to other salt hydrates, are related to a lack of stability due to phase segregation, a high degree of supercooling, and low thermal conductivity [16].

Researchers and developers' primary focus has been on eliminating or significantly reducing their associated barriers by obtaining a stable composition without phase segregation and with a reduced degree of supercooling. Phase segregation is commonly prevented by microencapsulation [24] with coating polymers [25,26], or by adding thickening agents, such as carboxymethyl cellulose with a content ranging from 1 to 5 wt% [27–29], xanthan rubber (0.25-1 wt%) [22], polyacrylamide (1-2 wt%) [30] or cellulose nanofibril (0.8 wt%) [31]. Supercooling is frequently reduced or eliminated by using nucleating agents [32], which improve the homogeneous crystallization ability of hydrates [33]. As nucleating agents, disodium hydrogen phosphate dodecahydrate ($Na_2HPO_4{\cdot}12H_2O$) [27–29,34], sodium metasilicate nonahydrate ($Na_2SiO_3{\cdot}9H_2O$) [29,34], tetrasodium pyrophosphate decahydrate ($Na_4P_2O_7{\cdot}10H_2O$) [29,30,34] or sodium tetraborate decahydrate ($Na_2B_4O_7{\cdot}10H_2O$) [29] are used. Other studies focus on supporting matrices for shape-stabilised composite PCM [35,36]. Additional, recent research evaluates how to enhance the thermal conductivity to increase the thermal power, above all during solid periods characterized by high thermal resistance. Thermal conductivity is usually enhanced by embedding powders and particles [37,38], such as copper powder [29], graphite powder [22], silver nanoparticles [39], aluminium nitride nanoparticles [40], copper nanoparticles [34] or expanded graphite [29,41,42]. Other studies even proposed novel heat exchange designs to overcome this low thermal power capacity, such as a screw heat exchanger [43] or rotating drum heat exchanger [44] in order to remove the solidified PCM layer in the heat exchanger surface, keeping the thermal power constant over time. As a result, all these advances and other improvements have resulted in a large portfolio of commercially available phase change compositions illustrated in Fig. 1b [15,19].

Despite supercooling being commonly attributed as a drawback [15,16], some studies have provided insights into using this property for long-term heat storage [45]. They use the terms undercooling, subcooling and supercooling alternatively since the melted liquid can cool down below its melting point without solidifying, remaining in a metastable state where the heat of fusion is not released [46,47]. In this supercooled stage, the liquid remains in a supersaturated state where the solution contains more solute than permitted by stable thermodynamic equilibrium, and homogeneous nucleation is not induced. So, the latent heat of material can be efficiently stored for long periods without latent heat losses until nucleation is initiated.

Stable supercooling could efficiently store low-carbon energy by melting the PCM, using solar energy or heat pumps throughout off-peak and low-carbon periods. After melting, the liquid material can supercool substantially below its melting point. As long as crystallization does not happen, the latent heat of the material can be stored for long periods without heat losses.

The ability of a supercooled compound to remain liquid at temperatures well below its melting point has been applied to different small-scale devices for warming foods [48] and drinks [49,50], portable heaters [51,52], pocket-sized heat packs [53,54] and body warmers [55,56]. They consist of a sealed envelope containing an aqueous solution with a trigger device. This trigger is able to initiate the nucleation and solidification of the liquid to release latent heat and can be used several times. Different studies have evaluated the reliability of triggers in promoting nucleation and crystallization. They can be classified into the following groups: seeding, local cooling (or supersaturation), impurities, electrical means, mechanical shocks, and agitation. However, the performance of different alternatives has shown discrepancies in the literature about their reliability [57]. Moreover, other experimental studies have evaluated the potential application of this material for solar TES by testing small-scale prototypes, initiated by Furbo et al. [58–60] and continued by Dannemand et al. [61–65], Englmair et al. [66–70] and Desgrosseilliers [71], among others.

Although several researchers and scientific publications have provided insights about supercooled liquids, the fundamentals for stable supercooling remain an open issue not always accompanied by relevant material investigations [19]. Existing discrepancies and research gaps are based on the fact that TES efficiency under cycling is not guaranteed by previous findings [*research gap 1*]; material segregation is not always correctly overcome [*research gap 2*]; stable supercooling is not as reliable as desired [*research gap 3*]; and crystallization is spontaneously triggered under inadequate boundary conditions or inaccessible under inappropriate material use [*research gap 4*]. Previous studies state that the stability of supercooled sodium acetate (SA, $NaCH_3COO$) aqueous solution cannot be ensured [72], showing that SA concentration of 54.85 wt% does not have stability after 20 cycles due mainly to the water loss during cycles, reducing thermal capacity from 194 to 179 kJ/kg [64], or even requiring concentration below the solubility curve of anhydrous salt to prevent precipitation [73]. Other studies to improve material stability by avoiding the evaporation of crystal water and phase segregation have reduced or even eliminated the subcooling potential of material [74]. It should also be noted that the understanding of crystallization is a longstanding issue in solid-state chemistry [47,75], remaining one of the most enigmatic processes in nature [76]. Additionally, the mechanisms to control reliable crystallization are challenging in technical applications [45], with discrepancies found in previous studies [57]. These are the main barriers that today limit their use in commercial heating applications. Supercooled SA solutions still need to be widely understood to efficiently support the pathway towards long-term heat storage systems to push domestic heating decarbonisation.

This research evaluates through a systematic experimental characterisation the physic and chemistry of the most promising supercooled liquid for long-term heat storage suitable for heating decarbonisation, based on SA. The aim is to clarify the existing discrepancies in the literature and identify the optimal material configuration and additional research needs required for a real application. The experimental methods were based on infrared thermography, differential scanning calorimetry (DSC), thermogravimetric analysis (TGA) and different experimental setups with different test tubes and containers monitored with thermocouples. Moreover, a small-scale experimental heat battery prototype was built and tested, integrating the most stable and reliable configuration to demonstrate its suitable operating conditions to support heating decarbonisation in a real environment. The results are critically compared with the existing literature contributions and confirm how SA solutions can achieve high thermal reliability, stable supercooling, reliable crystallization, and constant efficiency and stability under cycling without additional additives for long-term heat storage, which differs from previous studies. The main research contributions of this work are:

- Existing discrepancies in the literature about supercooled SA solutions are clarified, showing the fundamentals for an optimal material configuration. Despite previous studies showing that the thermal reliability and stability of SA aqueous solution as a supercooled liquid for heat storage cannot be guaranteed, this study demonstrates how through an appropriate encapsulation and sealing method, the

peritectic sodium acetate aqueous solution (p-SA at 58 wt%) can be used as a supercooled liquid for long-term heat storage with a stable melting temperature and latent heat capacity without any additional additive (addressing research gaps 1 and 2).
- The required boundary conditions for stable supercooling and the best available trigger mechanisms for reliable crystallization are highlighted, clarifying the discrepancies with previous studies (addressing research gaps 3 and 4).

These contributions pave the way for developing long-term thermal storage alternatives to support the building sector in the effort to decarbonise heating. The study demonstrates the potential benefits of supercooled liquids for long-term heat storage. Additionally, additional research needs for a wide deployment of this promising heat storage alternative in real applications are highlighted.

The paper is structured as follows. First, the materials and methods are detailed. Second, the results are provided and discussed through a systematic experimental evaluation divided into the following sections: evaluation of supercooling process through infrared thermography (3.1); supercooling stages in phase diagram showing the fundamentals and required boundary conditions for a functional material performance with long-term stability and reliability (3.2), additional requirements for stable supercooling in the metastable liquid zone (3.3); evaluation of maximum temperature required for heat storage in a real environment (3.4); validation of best available crystallization alternatives (3.5); evaluation of TES density (3.6); demonstration of thermal reliability, stability and storage efficiency of p-SA under cycling (3.7); and potential applications to support heating decarbonisation (3.8).

2. Materials and methods

This study experimentally analyses the optimal SA-based solution as a supercooled liquid for long-term heat storage. Materials and preparation are detailed in Section 2.1. Methods for experimental testing are defined in Section 2.2.

2.1. Materials

Sodium acetate trihydrate (SAT, $NaCH_3COO{\cdot}3H_2O$) (CAS 6131-90-4) with purity higher than 99.5 % from Sigma-Aldrich was employed. SAT has 60.3 % sodium acetate (SA) and 39.7 % water [19,40,77]. SA-based solutions were obtained from SAT by adding distilled water in order to achieve a SA concentration of 58 % (peritectic composition, p-SA) and 56 %. They are detailed in Table 1. The SAT-water mixtures were obtained by melting and stirring uniformly in sealed vials. A thermostatic water bath was used for melting.

Table 1
SA aqueous solutions tested.

ID	Name	SA content (wt %)	Water content (wt %)
SAT	Sodium acetate trihydrate	60.3 %	39.7 %
p-SA (58 wt %)	peritectic SA aqueous solution	58 %	42 %
SA (56 wt%)	SA aqueous solution	56 %	44 %

2.2. Experimental methods

Five experimental methods were used to systematically analyse the physic and chemistry of sodium acetate ($NaCH_3COO$) aqueous solutions. They are summarised in Table 2 and detailed below.

2.2.1. Infrared thermography

Thermal images in different stages of the supercooling and crystallization process were taken with a FLIR E5 infrared camera. This test was performed to understand the heat release during the crystallization growing process since the showed infrared temperatures are associated with material emissivity and may differ from the real temperatures.

2.2.2. Differential scanning calorimetry

Differential Scanning Calorimetry (DSC) was used to evaluate the melting point, latent heat capacity, supersaturation limit of supercooled samples and efficiency under cycling. DSC Q200 instrument from TA Instruments company was employed. The apparatus was calibrated using the melting temperatures and latent heat of standard certified reference material (Indio, In). Thermal analysis was performed using samples with a low mass between 4.50 and 10.00 mg to improve heat transfer and minimise thermal gradients within the sample [78]. All DSC samples were encapsulated in Tzero Pans (container of the sample material) with Tzero hermetic Lids (cap of the container). Measurements were carried out in a temperature range from −50 to 75 °C with a heat rate of 5 °C min^{-1}, under a purified nitrogen atmosphere with a flow rate of 50 mL min^{-1}.

2.2.3. Thermogravimetric analysis

Thermogravimetric analysis (TGA) was used to characterise the water content of SA solutions. SDT Q600 instrument from TA Instruments company was used, which provides simultaneous measurement of weight change (TGA) and differential heat flow. All samples with a mass of 15–25.00 mg were introduced in 90 μL alumina crucibles. Measurements were carried out in a temperature range of 25–110 °C with a heating rate of 5 °C min^{-1}, under a purified nitrogen atmosphere with a flow rate of 100 mL min^{-1}.

2.2.4. Experimental setup with thermocouples

An experimental setup with different test tubes and containers of the *p*-SA solution was carried out to evaluate the requirements and efficiency of stable supercooling (Fig. 2). The temperature oscillation of samples was measured with type T thermocouples, immersed in the sample and sealed to prevent water evaporation. A thermostatic water

Table 2
Experimental methods, targets, and properties evaluated.

Experimental methods	Targets	Property	Unit
Infrared thermography	Heat release during crystallization	Crystallization process	–
Differential Scanning Calorimetry (DSC)	Thermal application	Melting point	°C
		Supercooling	°C
		Supersaturation limit	°C
	Thermal storage capacity	Latent heat of phase change	kJ/kg
	Performance over several thermal cycles (Efficiency after thermal cycles)	Thermal reliability	%
Thermogravimetric analysis (TGA)	Degradation of material with the increase of temperature	Thermal stability or weight loss	%
Experimental setup with thermocouples	Material performance in a real environment	Requirements for stable supercooling	–
		Phase change transition range	°C
		Thermal response during crystallisation	°C
Test of crystallization alternatives	Heterogeneous crystallization	Crystallization reliability	–

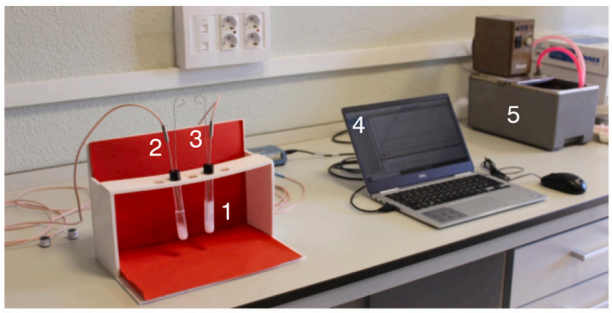

Experimental instruments:
(1) Samples in test tubes, (2) Thermocouples, (3) Trigger (contact-induced nucleation), (4) Data acquisition system, and (5) Thermostatic water bath.

Fig. 2. Experimental instruments for the characterisation of melting and crystallization process.

bath was used for heating and melting. This setup was used to analyse the following aspects:

-Requirements for stable supercooling in the metastable liquid zone. Different experimental tests of different fully-melted and partially-melted conditions were monitored;

-Phase change transition range in a real environment in order to identify the operating temperatures required for a fully-melted condition using domestic heat sources;

-Thermal response during crystallization after long-term storage periods. After different heat storage periods and activation temperatures, the thermal response was compared using the temperature difference (ΔT) between the sample and reference obtained with type T thermocouples.

Three identical samples were tested per experiment.

2.2.5. *Crystallization alternatives for heat release*

The boundary conditions for reliable crystallization were evaluated by testing all mechanisms for heterogeneous crystallization found in the literature and patents. The following crystallization methods were tested: seeding, local cooling, impurities, electrical means, mechanical shocks and agitation. They are summarised in Table 3. The complete procedure for each crystallization method is explained, discussed and compared with previous studies in section 3.5.

3. Results and discussion

The systematic experimental evaluation and characterisation of SA aqueous solution as a supercooled liquid for long-term heat storage is divided into eight sections. They are focused on the definition and characterisation of the supersaturation state, the material design and integration to avoid phase separation and spontaneous nucleation, the boundary conditions to achieve stable supercooling and a reliable heat release, the demonstration of thermal reliability, stability and efficiency of the p-SA composition, and the discussion of potential applications.

Table 3
Crystallization methods promote heterogeneous crystallization.

Methods	Definition
Seeding	Providing a stable solid crystal from the same material to promote crystallization
Local cooling	Displacing a portion of the material under the supersaturation limit curve
Impurities	Adding particles to be SA solution to modify the supersaturation limit curve
Electrical means	Application of the electric fields to promote nucleation
Mechanical shocks	Application of impact stress to trigger the crystallization
Agitation	Stirring to trigger the nucleation

3.1. *Supercooling process through infrared thermography*

The thermal energy storage process for long-term periods through supercooled liquid is illustrated in Fig. 3, including material melting (Fig. 3a), supercooling stage (Fig. 3b) and induced crystallization (Fig. 3c). Different infrared thermography sequences were taken to illustrate the heat storage process during each stage.

Fig. 3a illustrates the charging process (heat supply for TES). The salt hydrate undergoes a phase change from solid to liquid while absorbing heat, increasing its temperature. In Fig. 3b, the sample is cooled down to the supercooling stage, releasing sensible heat but remaining the latent heat since crystallization is not initiated. In this state, the melted material in a liquid state cools down below its melting point without solidifying and leaves it in a metastable state where the latent heat of fusion is not released. It is caused by the poor nucleating properties of the material [46,47] and could be controlled by different techniques [57]. Thus, latent heat of material could be stored for long-term periods, without latent heat losses, until the nucleation is triggered. Finally, Fig. 3c shows the crystallization and heat release process of the sample. A nucleation seed is added to the material (using a seed crystal in Fig. $3b_2$) to initiate the crystallization process and release all latent heat stored, increasing the material temperature as shown in the infrared thermography sequence (Fig. $3c_{1\text{-}4}$). In this process, material temperature is increased according to ambient temperature, in this case, up to 55 °C according to type T thermocouples measures.

3.2. *Supercooling stages in the phase diagram*

The behaviour of SAT and SA solutions in the supercooling stage is illustrated in Fig. 4, which contains the phase diagram of SA aqueous solutions (Fig. 4a) and the schemes (Fig. 4b) and photographs (Fig. 4c) of incongruent and congruent melting under different SA-water concentrations. The phase diagram of sodium acetate aqueous solution was created using experimental data from [79–82], and corroborated through own experimental measurements. The phase diagram also identifies the different states of the solution, with the identification of anhydrous salt and water vapour zone (A), liquid SA solution zone (B), liquid and SA trihydrate or metastable liquid SA solution zone (supersaturated) (C), anhydrous in liquid SA solution (D), solid SA trihydrate and anhydrous salt or metastable liquid SA solution with a precipitate of anhydrous salt (supersaturated) (E), ice and SA trihydrate or labile zone (supersaturated) (F), and peritectic composition (p-SA).

A supercooled liquid based on a salt hydrate consists of a supersaturated state. In this state, the solution contains more solute than permitted by stable thermodynamic equilibrium, and homogeneous nucleation is not induced [46]. This region is located between saturation and maximum supersaturation in the phase diagram and it is designated as the metastable liquid zone (zone C in Fig. 4a). The labile zone term is employed for an even more concentrated solution state where spontaneous crystallization is likely, though not guaranteed (Zone F in Fig. 4a). This supersaturated limit is not a sharply defined point since maximum supersaturation decreases with the level of impurities and other physical factors that encourage spontaneous nucleation [46,47]. For example, it was evidenced that by increasing the impurity level when in contact with steel components, the solution shifts the supersaturation limit from −24 °C to −9 °C [67]. Besides, the material and roughness of the container should be considered for appropriate supercooling stability. Previous studies have demonstrated that higher roughness of the metallic surface can reduce the supercooling degree, producing spontaneous crystallization [83]. Peng et al. [84] evaluated how the surface free energy affects the stable supercooling, showing that containers made of materials with lower surface free energy (e.g. stainless steel and polytetrafluoroethylene (PTFE)) are considered beneficial in stabilizing supercooling [84].

Pure SAT ($NaCH_3COO{\cdot}3H_2O$) has a SA concentration of 60.3 % and a water weight proportion of 39.7 %, similar to previous studies [40,85],

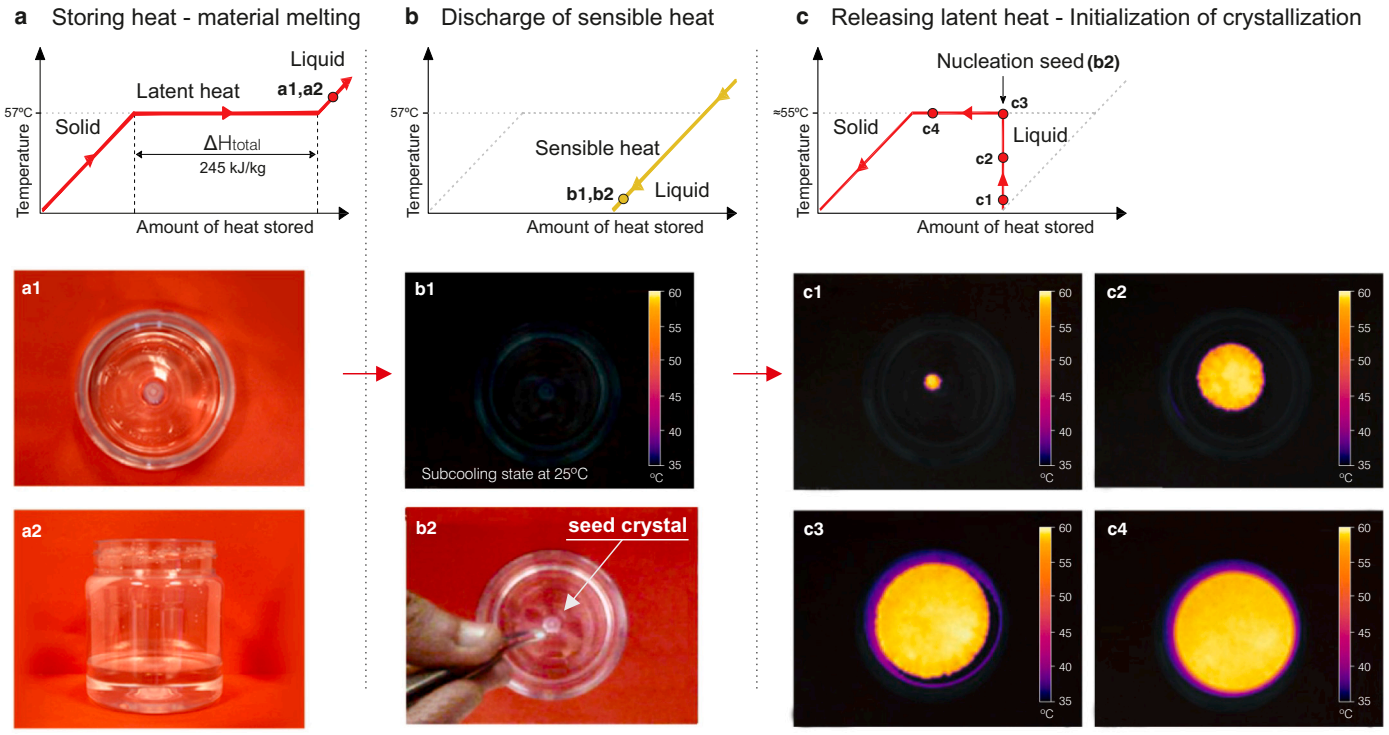

Fig. 3. Thermal energy storage process of sodium acetate (p-SA) solution with stable supercooling. a) storing heat – material melting. b) Discharge of sensible heat while latent heat is conserved and stored. c) releasing latent heat – initialization of crystallization.

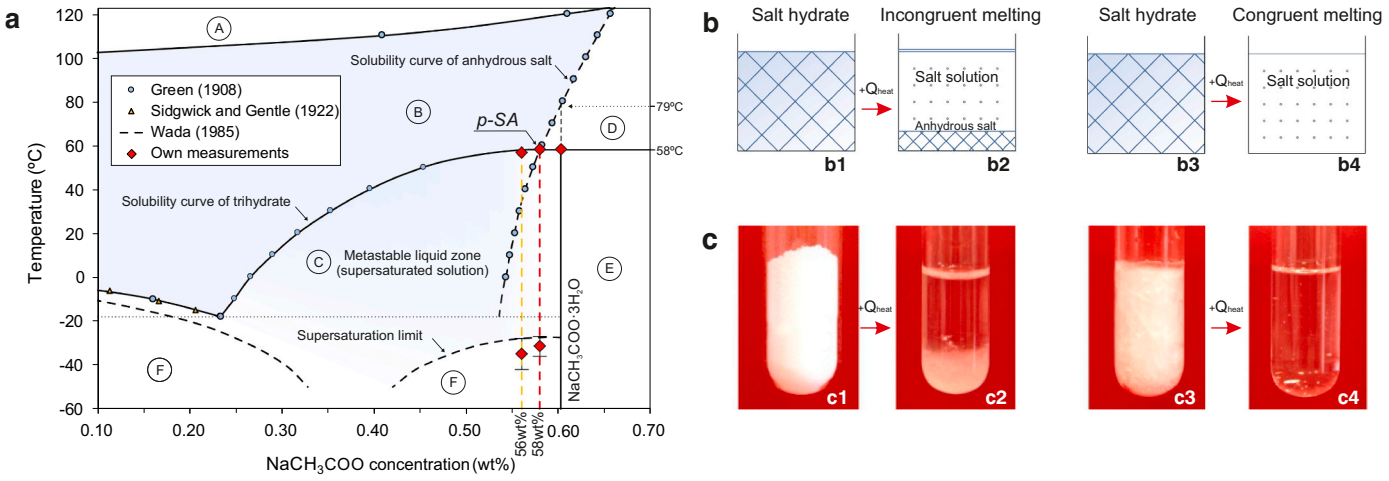

Fig. 4. Supercooling stages. a) Phase diagram of sodium acetate aqueous solution. b) Schematic sequence of the incongruent melting and congruent melting. c) Photographs of incongruent melting (SAT or SA at 60.28 wt%) and congruent melting (p-SA at 58 wt%).

and shows a melting temperature of 57.7 °C and a latent heat capacity of 284.5 kJ/kg in its first melting curve, with a standard deviation (SD) of 3.7. However, this composition is unstable after the first heating above 58 °C. It undergoes phase separation during melting, producing anhydrous salt and a peritectic SA solution (*p*-SA) containing 58 wt% of sodium acetate and 42 wt% water. This behaviour is illustrated in the diagrams Fig. 4b$_{1,2}$ and photograms Fig. 4c$_{1,2}$. Due to its higher density, the solid salt settles down at the bottom of the container, and it is unavailable for recombination with water during the reverse process of freezing [21]. It results in an irreversible and incongruent melting with phase segregation of anhydrous salt [19,77]. In this case, only heating above 79 °C, as indicated by the phase diagram (Fig. 4a), could avoid the presence of un-dissolved anhydrous salt. Nevertheless, adding a slight excess of water at or below the p-SA concentration (p-SA in Fig. 4a) avoids this problem, as illustrated in Fig. 4b3,4 and Fig. 4c3,4 [77]. Nevertheless, decreasing the SA solution concentration reduces the phase equilibrium temperature and latent heat capacity. This is further described in Section 4.6.

3.3. *Requirements for stable supercooling in the metastable liquid zone*

The boundary conditions for stable supercooling were evaluated through an experimental setup previously defined in section 2.2.4 using three test tubes containing the *p*-SA solution per experiment. Two experiments were tested: one with fully melted samples and another with partially melted samples. Heating and melting were conducted through a thermostatic water bath. Then, cooling curves were monitored with thermocouples, cooling down at ambient temperature. A partially

melted state was considered with an approximate liquid fraction between 80 % and 95 %.

The results of the experiment are illustrated in Fig. 6. The cooling curves of three samples fully melted samples are shown in red lines. The three partially melted samples are displayed with blue lines.

The results show that stable supercooling is based on the poor nucleating properties of SA solution after the material is fully melted. If the compound is partially melted, the remaining solid acts as a nucleating agent, crystalising and releasing the latent heat during the cooling process, with a relatively small degree of supercooling (Fig. 5b, blue line). Thus, it is essential to ensure a fully melted solution to ensure poor nucleating characteristics [21] for long-term energy conservation [86]. Once the material is fully melted, the salt solution would remain under a metastable liquid state, below the melting temperature, where the latent heat of fusion is not released until nucleation is induced.

3.4. Temperature required for heat storage

Because the material requires a complete melting state to ensure poor nucleation and stable subcooling, this section analyses the temperature needed in a real environment to achieve this fully-melted state. Fig. 6a shows the results of temperature evolution as a function of the time of three small-scale containers (experimental heat batteries) with samples of p-SA solution (SA 58 wt%). They are illustrated in three colours: black, red and orange. The aim is to evaluate the appropriate melting temperatures for long-term heat storage using domestic heat sources, such as electric heat pumps or solar energy sources.

The results show that the material achieves a fully-melted state at 57.5 °C. The three samples show almost a complete overlapping, following the same trend. Once fully melted, it cools below its melting point without solidifying, remaining in a metastable state where the heat of fusion is not released. These temperature results are even below those recently obtained by Li et al. [87], or Xu et al. [88], which studied the performance of a modified SAT for a stable transition (without subcooling) in a real environment and obtained a melting temperature range higher than 60 °C. Thus, it is demonstrated that the increase of water content to the p-SA concentration was able to maintain material stability and reduce phase change transition to a more appropriate range for domestic heat sources.

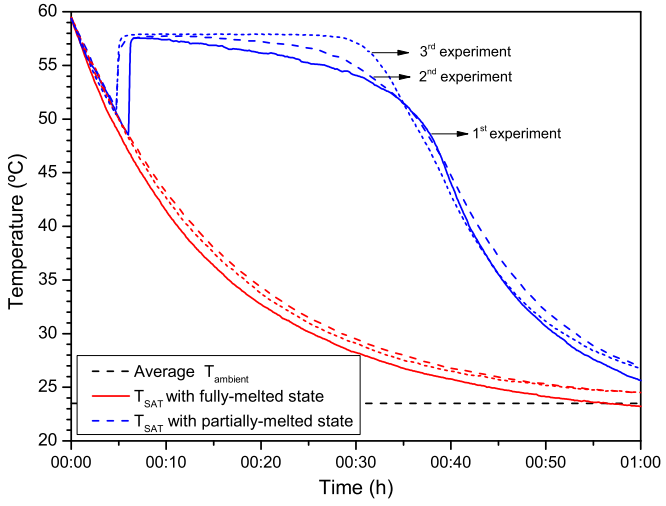

Fig. 5. The required boundary condition for stable supercooling in the metastable liquid zone. Cooling of p-SA solution with the material in a fully-melted state (red lines) and a partially-melted state (blue lines). (For interpretation of the references to colour in this figure legend, the reader is referred to the web version of this article.)

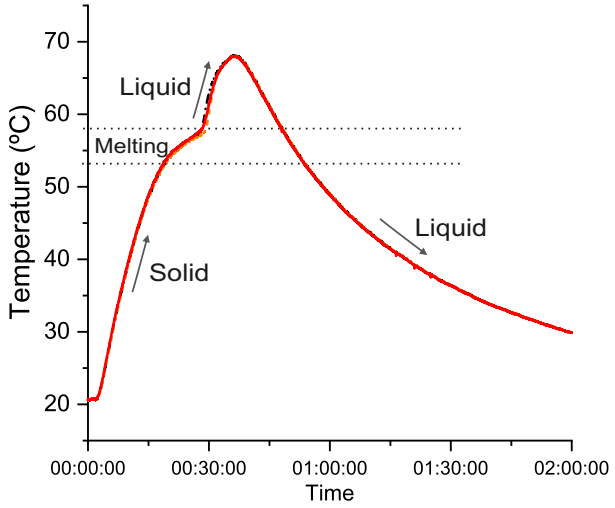

Fig. 6. Evaluation of maximum temperature to achieve a fully-melted state in a real environment. Melting curves of three experimental heat battery samples using p-SA solution as a supercooled liquid.

3.5. Crystallization alternatives for heat release

Understanding and controlling nucleation is a longstanding issue in crystallization and solid-state chemistry [47,75], and it remains one of the most enigmatic processes in nature [76]. Many patents over time and the continuous development of triggering mechanisms [66,89] indicate the continuing need for a simple, effective and reliable mechanism for activating crystallization. Common complaints are related to unintentionally crystallization activation and malfunction after a while [90]. The performance of the most common devices of a reliable heterogeneous crystallization is illustrated in Fig. 7.

Fig. 7a shows the process of heterogeneous crystallization using a trigger involving material melting, nucleation trigger and crystal growth. The trigger induces the driving forces to create of first nucleus or crystal, which initiates the crystal growth and total crystallization of the liquid. In most cases, this first crystal is produced by the presence of a foreign substance.

Several methods have been proposed in the literature and patented to trigger crystallization. They can be divided into the following groups: seeding, local cooling (or supersaturation), impurities, electrical means, mechanical shocks, and agitation. However, the performance of different alternatives has shown discrepancies in the literature about their reliability [57]. All of them have been experimentally tested in the lab, and the results compared with previous findings are summarised in Table 4. They are explained as follows.

- Seeding refers to providing a stable solid crystal from the same material to promote crystallization. In this case, the major issue for nucleation triggering by seeding is to keep or create the crystal. Two techniques can be found using this concept: contact-induced nucleation and storing seed crystals.
  Contact-induced nucleation consists of a manual open and closed valve (one-way valve) with a rod. When desired to use the stored heat, the valve is extracted while a portion of the solution adheres to the rod. This part of the rod is then dried with the surrounding microenvironment, evaporating the solvent from the salt solution and forming minute crystals, which will initiate the crystallization after reintroducing through the valve opening. Many patents can be found using this concept [48,50–52,56,91]. Even a novel automatic alternative based on this concept has been recently tested by Englmair et al. [66]. Our tests using this technique showed good reliability in triggering heterogeneous nucleation, as illustrated in Fig. 7b.

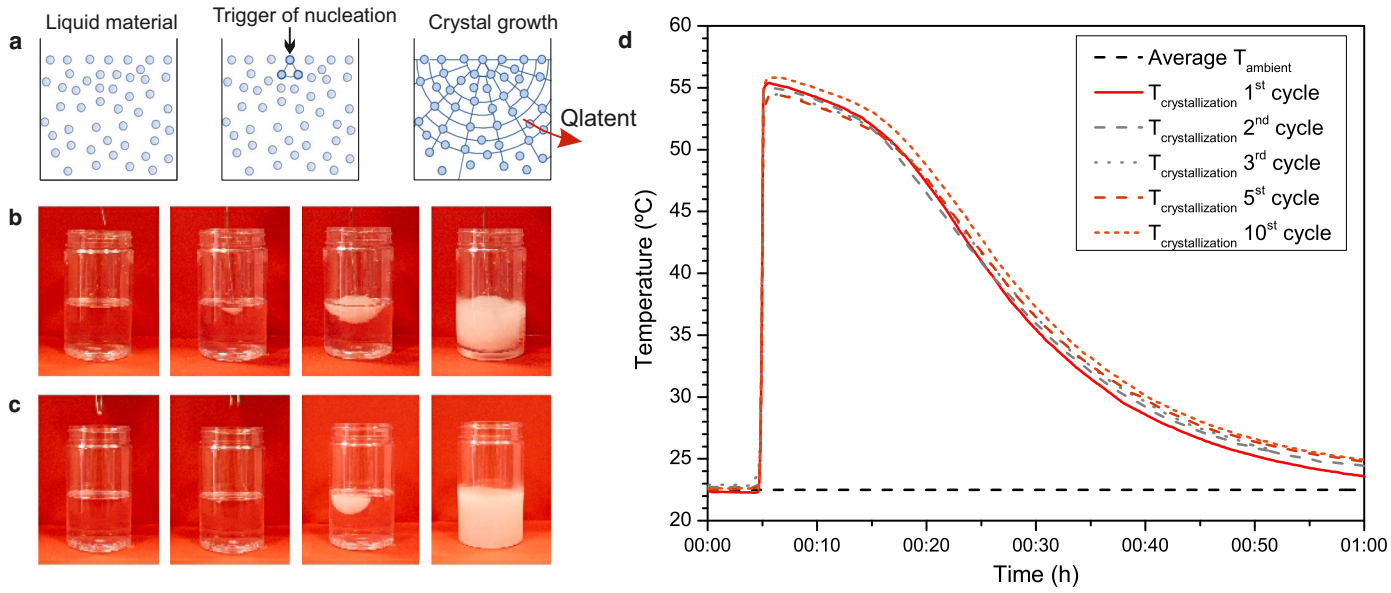

Fig. 7. Illustration and performance of crystallization alternatives. a, Schematic sequence of the crystallization process. b, Photographic sequence of crystallization by contact-induced nucleation. c, Photographic sequence of crystallization by adding a seed crystal. d, Crystallization process over the first ten cycles of a SA solution by triggering nucleation.

Table 4
Comparison of crystallization alternatives.

Methods	Existing studies and patents	Discrepancies	Results of experimental tests
Seeding	[48,50–52,56,66,73,90–98]	No	Nucleation
Local cooling	[58,64,67,99]	No	Nucleation
Impurities	[49,54,100–103]	Yes	Nucleation but modifying the supersaturation limit of the sample
Electrical means	[89,104–106]	Yes	No crystallization
Mechanical shocks	[94,107]	Yes	No crystallization
Agitation	[108,109]	Yes	No crystallization

Storing seed crystal is another commonly used technique, where heat is related after liquid contacting seed crystal to promote crystallization. Different patents have been found where they store crystals in a separate container [92,93] or retain them under pressure [73,90,94]. Günther et al. [95] demonstrated that the SA solution increases its melting point when applying high pressure. The most extended alternative to retaining crystals under pressure is based on embedded metallic trigger disks [96], in which minute crystals are harboured in submicron cracks or irregularities on the metallic devices. Crystals remain there during the material melting, and after flexing the device, they are released into the subcooled solution, initiating crystallization. The pressure created at the points of contact of the microscopic asperities prevents the crystal from expanding as the salt solution is heated above its melting temperature, thereby maintaining its crystalline phase [97]. The exposure of pressured crystal to the supercooled liquid is accomplished simply by flexing the device to the opposite position that holds the asperities together, so the crystal is no longer isolated, triggering crystallization. Other similar pressure mechanisms are spring-type triggers [97], or retaining crystals by applying a force to press two solid tightly together [98]. The tests carried out in the lab using this technique showed good reliability in triggering heterogeneous nucleation, as illustrated in Fig. 7c.

- Local cooling (or local supersaturation) is based on the displacement of a portion of the material under the supersaturation limit curve, where spontaneous crystallization is highly probable (zone F in Fig. 4a). The process is often called “cold finger” [99] and it has been previously demonstrated using Peltier elements [67] and the evaporation of liquid CO_2 [58,64]. They generate local cooling, or “a cold spot”, in the undercooled liquid and promote nucleation and crystallization. This technique was experimentally tested using DSC cycles. Samples of SA solutions were introduced in a hermetic pan for DSC analysis, and crystallization was forced by freezing the material below the maximum supersaturated limit, in the labile zone, where spontaneous crystallization occurs. These tests, further detailed in supplementary material, showed good reliability in triggering crystallization.
- Impurities consist of adding particles to the SA solution, contacting the supercooled salt solution, and initiating crystallization and heat release. Many different alternatives and patterns have been found following this technique based on scraping the inside of a container with a wire [49]; rough bodies within the solution [54,100], which are scraped together in order to cause friction between the contacting surfaces and activate crystallization, dry particles adhering to a support [101,102], or abrasive particles of aluminium oxide affixed to flexible screens [103]. They all follow the same principle: when the trigger is manipulated, the particles or impurities are released. This concept has been tested with different samples, showing poor reliability and even modifying the supersaturation limit of the sample. The metastable liquid zone, where supercooling is stable, decreases with the level of impurities [46,47]. So, this approach should be limited to avoid alterations in the supercooling stability.
- Electrical triggers refer to the application of the electric fields to promote nucleation. Electric fields to promote nucleation of SA solution were tested by [104] and carried on in later works in [105,106]. However, Sakurai and Sano [89] evidenced that the electric field was not the driving force of nucleation, concluding that successful scenarios were derived from the dehydration of clusters from the anode. This effect was confirmed by our tests, where the application of different voltages and tensions didn't show any nucleation activity.
- Mechanical shocks are related to the effect of impact stress to trigger material crystallization. In this area, ultrasound waves have been

tested with successful crystallization but unreliable nucleation probability at a concentration above SA 55 wt% [107]. Other authors even refer that crystallization failed by using ultrasonic waves [94]. The results of our tests using an ultrasonic bath at different intensities didn't crystalise the samples.

- Agitation refers to the effect of stirring to trigger the nucleation. Previous studies have only proved that the process of agitation can reduce supercooling of salt hydrates [108,109]. So, this technique can influence the nucleation of some aqueous salt solutions, but it is not guaranteed. The results using this technique didn't show any nucleation.

After the experimental evaluation and testing of the aforementioned techniques, seeding and local cooling were identified as the best suitable strategies to trigger crystallization in SA solutions. When crystallization is initiated, the material releases all stored latent heat, achieving a temperature of approximately 55 °C, as shown in Fig. 7d. However, they should be correctly applied and used to ensure successful and reliable control of heterogeneous nucleation. For example, in the case of seeding by retaining crystals under pressure, the pressure should be guaranteed during high-temperature periods to avoid the total melting of retained crystals and inactivity. An inadequate trigger activation at a high temperature will release the pressurised crystals, inactivating the mechanism [90]. On the other hand, the tests developed with impurities, electrical means, mechanical shocks, and agitation didn't show reliability in triggering nucleation in supercooled SA solutions.

3.6. Thermal energy storage density

The latent heat capacity and melting temperature of different SA aqueous solutions were evaluated through DSC measurements, which are reported in Table 5. Additionally, Fig. 8 shows the comparison of our measurements with those found in the literature by different authors: Tamme et al. [110], Araki et al. [111], Dannemand et al. [64] and Zhao et al. [27].

The results show how the latent heat capacity is reduced by decreasing the SA solution concentration, from 284.5 kJ/kg for the SAT aqueous concentration to 246 kJ/kg and 225.4 kJ/kg for p-SA (58 wt%) and SA (56 wt%) concentrations, respectively. Additionally, the melting temperature decreases with increased water concentration, as shown in the phase diagram in Fig. 4a.

The slight differences among reported latent heat values, including those obtained in this work (Fig. 8), could be explained in terms of their different experimental procedures. Other authors have used different instruments for their measurements (DSC vs twin calorimeter of the heat transfer type). Moreover, the integration procedure, selected baseline, or temperature range for the curve integration might provide a slightly different result, as shown in the literature [78]. These deviations in the latent heat values have been previously reported by other authors [64,112].

3.7. Thermal reliability, stability and storage efficiency of p-SA

This section evaluates the thermal reliability, stability and storage efficiency of p-SA for heat storage applications. Some previous studies refer that the stability of SA solution is not ensured, showing that SA concentration of 54.85 wt% (SAT with 9 wt% of additional water) does not have stability after 20 cycles, reducing thermal capacity from 194 to

Table 5
Results of DSC measurements.

SA aqueous solutions	Enthalpy (kJ/kg)	Melting (°C)
Pure SAT (60.2 wt%)	284.5	57.7
p-SA (58 wt%)	246.0	57.7
SA (56 wt%)	225.4	56.7

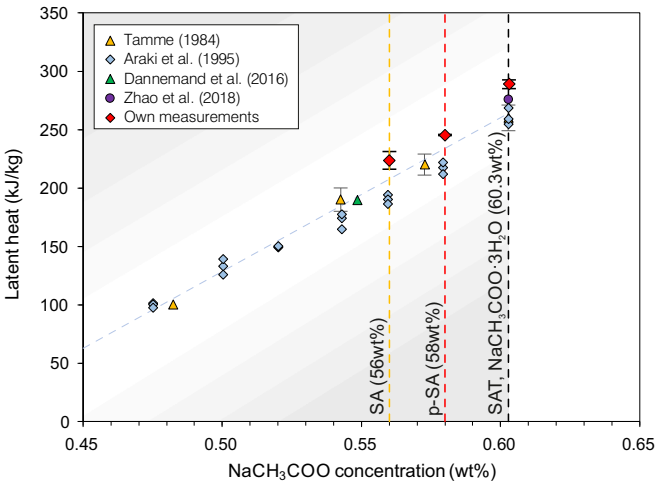

Fig. 8. Latent heat of fusion of different SA aqueous solutions.

179 kJ/kg [64] or even requiring concentration below the solubility curve of anhydrous salt to prevent precipitation (SA below 54.25 wt% or corresponding to trihydrate with more than 10 % additional water by weight) [73]. However, it should be considered that SA aqueous solution can lose its water of crystallization with the surrounding microenvironment, even with the air inside the sealed container at a temperature lower than the melting point. Thus, a suitable encapsulation method and surface sealing should be employed to avoid water loss and associated phase segregation, as demonstrated below.

Table 6 shows the results of the DSC measurements in the first and tenth thermal cycle of p-SA solution (58 wt%) using different encapsulation methods: sealed and unsealed. The sealed sample was based on the encapsulation of p-SA in a hermetic pan for DSC cycling, in which crystallization was forced during cycling by cooling the material until the maximum supersaturated limit, in the labile zone, where spontaneous crystallization occurs. The unsealed scenario consists of a p-SA sample located in a test tube containing the solution and air, in which a contact-induced nucleation mechanism triggered the crystallization. After cycling, the sample was collected and tested in the DSC instrument. Additionally, the DSC result of SAT in its first thermal cycle is provided as a reference value.

The DSC results in Table 6, and further detailed in the supplementary material, show that the p-SA composition has stable and congruent thermal reliability and stability after ten cycles under an appropriate sealing method, maintaining its properties. However, a lower SA concentration of 56 wt% was obtained in an unsealed sample after ten cycles, decreasing the latent heat capacity from 246 kJ/kg to 225.4 kJ/kg. In this case, the initial SA concentration decreased throughout the thermal cycling due to the water loss in the surrounding microenvironment.

The DSC heating curves of samples reported in Table 6 are illustrated in Fig. 9a. The reference DSC curve of pure SAT (60.28 wt%) in the first thermal cycle is shown as a black curve. Red curves show the performance of the p-SA solution at 58 wt% (*p*-SA) in the first and tenth thermal cycle, using a sealed encapsulation method during cycling. The blue curve illustrates the performance of the same *p*-SA solution after ten thermal cycles in the unsealed scenario. These measurements demonstrate that the p-SA composition under sealed conditions has high reliability and stability under thermal cycling, showing the same heat flow curve in DSC tests (red curves – Fig. 9a).

The stability of the sealed p-SA solution was also collected and illustrated in Fig. 9b. It shows the latent heat capacity and melting temperature of the p-Sa solution during 20 thermal cycles. These results show how the p-SA solution maintains its latent heat capacity and melting temperature at a mean constant value of 245 kJ/kg and 57 °C,

Table 6
Water content, latent heat of fusion and melting point of pSA solutions before and after ten cycles in sealed and unsealed scenarios.

	1st cycle			10th cycle			
	SA (wt%)	Enthalpy (J/g)	Melting (°C)	Water (wt%)	Enthalpy (J/g)	Melting (°C)	DSC Curve in Fig. 9a
Pure SAT	60.28	284.5	57.67				Pure SAT
p-SA (sealed)	58.0	246.0	57.72	58.0	244.5	57.89	p-SA (sealed cycle)
p-SA (unsealed)	58.0	246.0	57.72	56.0	225.4	56.71	p-SA (unsealed cycle)

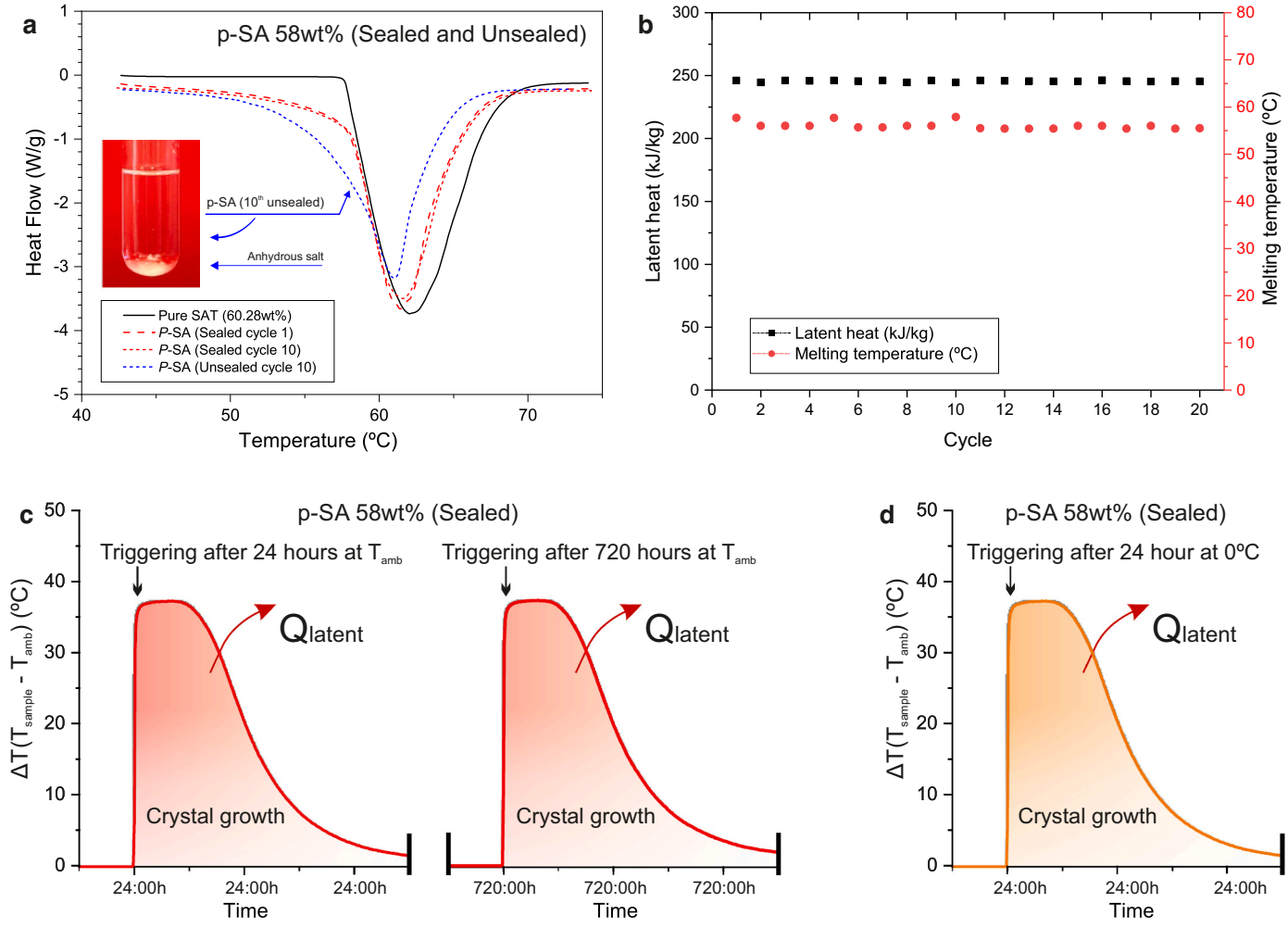

Fig. 9. Thermal reliability, stability and reliability of p-SA. a, DSC heating curves of pure SAT and p-SA solutions (58 wt%) with sealed and unsealed conditions before and after ten cycles. b, Stability of sealed p-SA sample during 20 DSC cycles. c, Delta temperature during heat release at 20 °C after different storage periods. d, Delta temperature during heat release at 0 °C after 24 h.

respectively.

Additionally, the reliability of the thermal response of p-SA after long-term storage periods is evaluated in Fig. 9c and d, which show the heat release curve as a temperature difference (ΔT) between the sample and a reference. Three p-SA samples were tested, encapsulated in different small-scale containers and stored in supercooled liquid form. The samples were activated after different storage periods and ambient temperatures to release all stored heat. The first and second samples in Fig. 9c were triggered after 24 h and 720 h (one month) at ambient temperature, approximately 21 °C, releasing all latent heat. The third sample in Fig. 9d shows the heat release at 0 °C after 24 h. The results show that all samples showed the same behaviour during the heat release along the different storage temperatures and periods, maintaining almost the same area under the thermal response curve.

The study demonstrates how heating decarbonisation can be efficiently supported using the p-SA composition through an appropriate encapsulation and sealing method. The appropriate encapsulation method allows the material to efficiently store thermal energy without latent heat losses whenever the solution operates in the temperature range between saturation and maximum supersaturation limit (metastable liquid zone). Thus, the material can be efficiently used for long-term heat storage with a stable melting temperature of 57 °C, a constant latent heat storage capacity of 245 kJ/kg and a volumetric storage density of 314 MJ/m^3. These results confirm the viability of this supercooled liquid for heat storage applications, clarifying existing discrepancies and opening a research pathway towards promising heat storage technologies. Storage temperatures enable the effective combination with heat pumps or solar technologies, considerably reducing carbon emissions and fulfilling climate targets, as discussed in the next section.

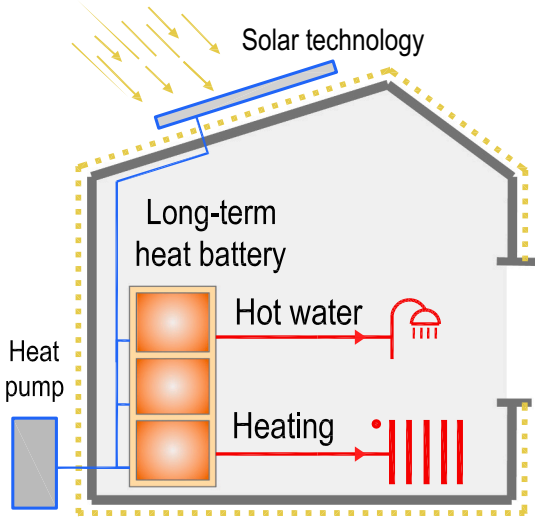

Fig. 10. The potential application of supercooled liquids according to common domestic heat sources to support heating decarbonisation.

3.8. Potential applications to support heating decarbonisation

The potential applications of the p-SA solution to support heating decarbonisation are illustrated in Fig. 10. It represents the use of a modulated TES system for hot water and/or space heating, which can be integrated with different heat sources alternatives. Application alternatives can be grouped into two main categories: electricity-based heating systems (heat pumps) or solar-based technologies (such as photovoltaic panels or solar collectors). The p-SA solution, with a phase change transition between 53 °C and 57.5 °C (Fig. 6), can be efficiently integrated to support smart demand response strategies in heating electrification using heat pumps or increase the share of solar energy for a long-term period. In all these applications, the TES unit will allow the better integration of renewable sources by solving the mismatch between demand and resource availability periods. Moreover, high-capacity TES systems would reduce the investment cost of renewable energy installations because of the contribution of TES along peak load demand periods without renewable energy supply [14].

4. Conclusions

This study experimentally analyses the promising supercooled liquid based on sodium acetate (SA) for long-term heat storage to support heating decarbonisation. The study provides novel insights into existing discrepancies in the literature through a systematic experimental evaluation, showing the fundamentals for efficient material design to avoid phase separation and spontaneous nucleation, and the necessary boundary conditions for proper material use.

Despite previous studies showing that the thermal reliability and stability of SA aqueous solution as a supercooled liquid for heat storage cannot be guaranteed, this experimental results demonstrate that the peritectic composition of SA solution (p-SA 58 wt%), through an appropriate encapsulation and sealing method, can be efficiently used for long-term thermal energy storage, with a stable melting temperature of 57 °C, appropriate for domestic heat sources. It is demonstrated that thermal reliability, stability and efficiency are maintained under cycling without any additional additive, with a constant latent heat storage capacity of 245 kJ/kg and a volumetric storage density of 314 MJ/m^3. The material can store thermal energy without latent heat losses, as far as the solution is totally melted and operating in the temperature range between saturation and maximum supersaturation limit (metastable liquid zone).

The analysis also shows that local cooling and retaining seed crystals through high pressure remain the fundamental principles towards successful crystallization. However, pressure mechanisms to retain crystals should be secured during high-temperature periods to avoid total melting of crystals and inactivity.

It was also demonstrated that the material behaviour in a real environment achieves a fully-melted state below 57.5 °C, below the maximum supply temperature of domestic heat technologies. Moreover, the thermal response of the material during crystallization showed the same performance after different storage periods and from different activation temperatures.

This novel storage concept based on the supercooled peritectic SA solution opens a new generation of promising heat storage technologies. Further research is required to evaluate the material's useful life in a relevant environment, involving a higher number of cycles, compatibility with other materials, corrosion performance, pressure conditions and heat exchange designs. Additionally, further studies could identify novel triggering techniques through local pressurization, modifying the solubility and supersaturation curves of a portion of p-SA solution to promote nucleation in a simple, effective, and reliable way.

Data availability

Data supporting this analysis, including the numbers behind the tables and figures, are available to any interested parties as online supplementary material to this paper. Any intermediate data not available from the sources are available from the authors on request.

CRediT authorship contribution statement

Jesus Lizana: Conceptualization, Data curation, Formal analysis, Investigation, Methodology, Software, Visualization, Writing – original draft. **Pedro E. Sanchez-Jimenez:** Data curation, Funding acquisition, Methodology, Resources, Supervision, Writing – original draft. **Ricardo Chacartegui:** Data curation, Funding acquisition, Methodology, Project administration, Resources, Supervision, Writing – original draft. **Jose A. Becerra:** Data curation, Methodology, Project administration, Supervision, Writing – review & editing. **Luis A. Perez-Maqueda:** Conceptualization, Formal analysis, Funding acquisition, Investigation, Methodology, Project administration, Writing – review & editing.

Declaration of competing interest

The authors declare that they have no known competing financial interests or personal relationships that could have appeared to influence the work reported in this paper.

Data availability

Data will be made available on request.

Acknowledgements

The authors gratefully acknowledge the Spanish Ministry of Science and Innovation's financial support via a Juan de la Cierva Postdoctoral Fellowship granted to Jesús Lizana (FJC2019-039480-I). Financial support from Project CTQ2017-83602-C2-1-R (MINECO-FEDER) and Project 201960E092 (INTRAMURAL-CSIC) is acknowledged. This research was also supported by the European Union's Horizon 2020 research and innovation programme under the Marie Skłodowska-Curie grant agreement No. 101023241.

Appendix A. Supplementary data

Supplementary data to this article can be found online at https://doi.org/10.1016/j.est.2022.105584.

References

[1] IPCC, Climate Change 2022. Mitigation of Climate Change. Working Group III Contribution to the Sixth Assessment Report of the Intergovernmental Panel on Climate Change, 2022.

[2] IPCC, IPCC Sixth Assessment Report. Chapter 9: Buildings, 2020, https://doi.org/10.1109/TSG.2017.2673783.Chapter.

[3] International Energy Agency, Transition to Sustainable Buildings. Strategies and Opportunities to 2050, OECD/IEA, 2013, https://doi.org/10.1787/9789264202955-en.

[4] R. Gross, R. Hanna, Path dependency in provision of domestic heating, Nat. Energy 4 (2019) 358–364, https://doi.org/10.1038/s41560-019-0383-5.

[5] E. McKenna, M. Thomson, High-resolution stochastic integrated thermal-electrical domestic demand model, Appl. Energy 165 (2016) 445–461, https://doi.org/10.1016/j.apenergy.2015.12.089.

[6] C. Mitchell, Momentum is increasing towards a flexible electricity system based on renewables, Nat. Energy 1 (2016), https://doi.org/10.1038/nenergy.2015.30.

[7] J. Lizana, D. Friedrich, R. Renaldi, R. Chacartegui, Energy flexible building through smart demand-side management and latent heat storage, Appl. Energy 230 (2018) 471–485, https://doi.org/10.1016/j.apenergy.2018.08.065.

[8] W. Heitkoetter, B.U. Schyska, D. Schmidt, W. Medjroubi, T. Vogt, C. Agert, Assessment of the regionalised demand response potential in Germany using an open source tool and dataset, Adv. Appl. Energy 1 (2021), 100001, https://doi.org/10.1016/j.adapen.2020.100001.

[9] Z. Wang, M. Sun, C. Gao, X. Wang, B.C. Ampimah, A new interactive real-time pricing mechanism of demand response based on an evaluation model, Appl. Energy 295 (2021), 117052, https://doi.org/10.1016/j.apenergy.2021.117052.

[10] Y. Chen, P. Xu, Z. Chen, H. Wang, H. Sha, Y. Ji, Y. Zhang, Q. Dou, S. Wang, Experimental investigation of demand response potential of buildings: combined passive thermal mass and active storage, Appl. Energy 280 (2020), 115956, https://doi.org/10.1016/j.apenergy.2020.115956.

[11] X. Jin, F. Wu, T. Xu, G. Huang, H. Wu, X. Zhou, D. Wang, Y. Liu, A.C. Lai, Experimental investigation of the novel melting point modified phase-change material for heat pump latent heat thermal energy storage application, Energy 216 (2021), 119191, https://doi.org/10.1016/j.energy.2020.119191.

[12] A.S. Gaur, D.Z. Fitiwi, J. Curtis, Heat pumps and our low-carbon future: a comprehensive review, Energy Res. Soc. Sci. 71 (2021), 101764, https://doi.org/10.1016/j.erss.2020.101764.

[13] E. Osterman, U. Stritih, Review on compression heat pump systems with thermal energy storage for heating and cooling of buildings, J. Energy Storage 39 (2021), https://doi.org/10.1016/j.est.2021.102569.

[14] J. Lizana, R. Chacartegui, A. Barrios-Padura, C. Ortiz, Advanced low-carbon energy measures based on thermal energy storage in buildings: a review, Renew. Sust. Energ. Rev. 82 (2018) 3705–3749, https://doi.org/10.1016/j.rser.2017.10.093.

[15] J. Lizana, R. Chacartegui, A. Barrios-Padura, J.M. Valverde, Advances in thermal energy storage materials and their applications towards zero energy buildings: a critical review, Appl. Energy 203 (2017) 219–239, https://doi.org/10.1016/j.apenergy.2017.06.008.

[16] J. Lizana, R. Chacartegui, A. Barrios-Padura, J.M. Valverde, C. Ortiz, Identification of best available thermal energy storage compounds for low-to-moderate temperature storage applications in buildings, Mater. Constr. 68 (2018) 1–35, https://doi.org/10.3989/mc.2018.10517.

[17] G. Alva, L. Liu, X. Huang, G. Fang, Thermal energy storage materials and systems for solar energy applications, Renew. Sust. Energ. Rev. 68 (2017) 693–706, https://doi.org/10.1016/j.rser.2016.10.021.

[18] T. Khadiran, M.Z. Hussein, Z. Zainal, R. Rusli, Advanced energy storage materials for building applications and their thermal performance characterization: a review, Renew. Sust. Energ. Rev. 57 (2016) 916–928, https://doi.org/10.1016/j.rser.2015.12.081.

[19] M. Kenisarin, K. Mahkamov, Salt hydrates as latent heat storage materials: thermophysical properties and costs, Sol. Energy Mater. Sol. Cells 145 (2016) 255–286, https://doi.org/10.1016/j.solmat.2015.10.029.

[20] H. Mehling, L.F. Cabeza, Heat and Cold Storage With PCM. An up to Date Introduction Into Basics and Applications, Springer, 2008.

[21] A. Sharma, V.V. Tyagi, C.R. Chen, D. Buddhi, Review on thermal energy storage with phase change materials and applications, Renew. Sust. Energ. Rev. 13 (2009) 318–345, https://doi.org/10.1016/j.rser.2007.10.005.

[22] M. Dannemand, J.B. Johansen, S. Furbo, Solidification behavior and thermal conductivity of bulk sodium acetate trihydrate composites with thickening agents and graphite, Sol. Energy Mater. Sol. Cells 145 (2016) 287–295, https://doi.org/10.1016/j.solmat.2015.10.038.

[23] K.E. N'Tsoukpoe, H. Liu, N. Le Pierrès, L. Luo, A review on long-term sorption solar energy storage, Renew. Sust. Energ. Rev. 13 (2009) 2385–2396, https://doi.org/10.1016/j.rser.2009.05.008.

[24] W. Su, J. Darkwa, G. Kokogiannakis, Review of solid-liquid phase change materials and their encapsulation technologies, Renew. Sust. Energ. Rev. 48 (2015) 373–391, https://doi.org/10.1016/j.rser.2015.04.044.

[25] J. Huang, T. Wang, P. Zhu, J. Xiao, Preparation, characterization, and thermal properties of the microencapsulation of a hydrated salt as phase change energy storage materials, Thermochim. Acta 557 (2013) 1–6, https://doi.org/10.1016/j.tca.2013.01.019.

[26] Q. Xiao, J. Fan, L. Li, T. Xu, W. Yuan, Solar thermal energy storage based on sodium acetate trihydrate phase change hydrogels with excellent light-to-thermal conversion performance, Energy 165 (2018) 1240–1247, https://doi.org/10.1016/j.energy.2018.10.105.

[27] L. Zhao, Y. Xing, X. Liu, Y. Luo, Thermal performance of sodium acetate trihydrate based composite phase change material for thermal energy storage, Appl. Therm. Eng. 143 (2018) 172–181, https://doi.org/10.1016/j.applthermaleng.2018.07.094.

[28] J. Mao, P. Hou, R. Liu, F. Chen, X. Dong, Preparation and thermal properties of SAT-CMC-DSP/EG composite as phase change material, Appl. Therm. Eng. 119 (2017) 585–592, https://doi.org/10.1016/j.applthermaleng.2017.03.097.

[29] M. Jinfeng, D. Xian, H. Pumin, L. Huiliang, Preparation research of novel composite phase change materials based on sodium acetate trihydrate, Appl. Therm. Eng. 118 (2017) 817–825, https://doi.org/10.1016/j.applthermaleng.2017.02.102.

[30] Y. Wang, K. Yu, H. Peng, X. Ling, Preparation and thermal properties of sodium acetate trihydrate as a novel phase change material for energy storage, Energy 167 (2019) 269–274, https://doi.org/10.1016/j.energy.2018.10.164.

[31] Z. Shen, S. Kwon, H.L. Lee, M. Toivakka, K. Oh, Enhanced thermal energy storage performance of salt hydrate phase change material: effect of cellulose nanofibril and graphene nanoplatelet, Sol. Energy Mater. Sol. Cells 225 (2021), 111028, https://doi.org/10.1016/j.solmat.2021.111028.

[32] X. Zhou, X. Zhang, Q. Zheng, Composite phase change materials with heat transfer self-enhancement for thermal energy storage, Sol. Energy Mater. Sol. Cells 217 (2020), 110725, https://doi.org/10.1016/j.solmat.2020.110725.

[33] M.M. Farid, A.M. Khudhair, S.A.K. Razack, S. Al-Hallaj, A review on phase change energy storage: materials and applications, Energy Convers. Manag. 45 (2004) 1597–1615, https://doi.org/10.1016/j.enconman.2003.09.015.

[34] W. Cui, Y. Yuan, L. Sun, X. Cao, X. Yang, Experimental studies on the supercooling and melting/freezing characteristics of nano-copper/sodium acetate trihydrate composite phase change materials, Renew. Energy 99 (2016) 1029–1037, https://doi.org/10.1016/j.renene.2016.08.001.

[35] D.G. Atinafu, C. Wang, W. Dong, X. Chen, M. Du, H. Gao, G. Wang, In-situ derived graphene from solid sodium acetate for enhanced photothermal conversion, thermal conductivity, and energy storage capacity of phase change materials, Sol. Energy Mater. Sol. Cells 205 (2019), 110269, https://doi.org/10.1016/j.solmat.2019.110269.

[36] D.L. Feng, Y.Y. Zang, P. Li, Y.H. Feng, Y.Y. Yan, X.X. Zhang, Polyethylene glycol phase change material embedded in a hierarchical porous carbon with superior thermal storage capacity and excellent stability, Compos. Sci. Technol. 210 (2021) 1–25, https://doi.org/10.1016/j.compscitech.2021.108832.

[37] E.-B.S. Mettawee, G.M.R. Assassa, Thermal conductivity enhancement in a latent heat storage system, Sol. Energy 81 (2007) 839–845.

[38] B. Eanest Jebasingh, A. Valan Arasu, A comprehensive review on latent heat and thermal conductivity of nanoparticle dispersed phase change material for low-temperature applications, Energy Storage Mater. 24 (2020) 52–74, https://doi.org/10.1016/j.ensm.2019.07.031.

[39] B.M.L. Garay Ramirez, C. Glorieux, E.S. Martin Martinez, J.J.A. Flores Cuautle, Tuning of thermal properties of sodium acetate trihydrate by blending with polymer and silver nanoparticles, Appl. Therm. Eng. 62 (2014) 838–844, https://doi.org/10.1016/j.applthermaleng.2013.09.049.

[40] P. Hu, D.J. Lu, X.Y. Fan, X. Zhou, Z.S. Chen, Phase change performance of sodium acetate trihydrate with AlN nanoparticles and CMC, Sol. Energy Mater. Sol. Cells 95 (2011) 2645–2649, https://doi.org/10.1016/j.solmat.2011.05.025.

[41] H.K. Shin, M. Park, H.Y. Kim, S.J. Park, Thermal property and latent heat energy storage behavior of sodium acetate trihydrate composites containing expanded graphite and carboxymethyl cellulose for phase change materials, Appl. Therm. Eng. 75 (2015) 978–983, https://doi.org/10.1016/j.applthermaleng.2014.10.035.

[42] S. Wu, T. Yan, Z. Kuai, W. Pan, Thermal conductivity enhancement on phase change materials for thermal energy storage: a review, Energy Storage Mater. 25 (2020) 251–295, https://doi.org/10.1016/j.ensm.2019.10.010.

[43] V. Zipf, A. Neuhäuser, D. Willert, P. Nitz, S. Gschwander, W. Platzer, High temperature latent heat storage with a screw heat exchanger: design of prototype, Appl. Energy 109 (2013) 462–469, https://doi.org/10.1016/j.apenergy.2012.11.044.

[44] J. Tombrink, H. Jockenhöfer, D. Bauer, Experimental investigation of a rotating drum heat exchanger for latent heat storage, Appl. Therm. Eng. 183 (2021), https://doi.org/10.1016/j.applthermaleng.2020.116221.

[45] A. Safari, R. Saidur, F.A. Sulaiman, Y. Xu, J. Dong, A review on supercooling of phase change materials in thermal energy storage systems, Renew. Sust. Energ. Rev. 70 (2017) 905–919, https://doi.org/10.1016/j.rser.2016.11.272.

[46] G.A. Lane, Crystallization, in: Solar Heat Storage: Latent Heat Material. Volume I: Background and Scientific Principles, CRC Press. Taylor & Francis Group, 2018.

[47] F.Grases Freixedas, A.Costa Bauzá, O. Söhnel, Cristalización en disolución: conceptos básicos, Editorial Reverté, 2000.

[48] C. Cronenberg, S.M.B.Von Szczawinski, Device for Retaining Heat in Foods, U.S. Patent 549959, 1895.

[49] D.F. Othmer, Valveless Chemical Heater, US Patent No 2220777, 1940.

[50] J.H. Layer, K. Solovay, T.P. Jacobs, Apparatus, Systems and Methods for Warming Materials, U.S. Patent 2004/0065314, 2004.

[51] J. Stanley, G.L. Hoerner, Chemical Heater, U.S. Patent No 1384747, 1921.

[52] H.G. Lewis, Heat-storage Battery U.S. Patent No 1433010, 1922.

[53] J. Stanley, G.L. Hoerner, Reusable Heat Pack Containing Supercooled Solution and Means for Activating Same, U.S. Patent No 4077390, 1978.

[54] F. Heiliger, Thermophore, US Patent No 708549, 1902.

[55] C. Harris, Infant Heel Warmer, U.S. Patent 2005/022846, 2005.

[56] R.S. Ferguson, Valve Mechanism for Heat Flasks, U.S. Patent No 1915523, 1933, https://doi.org/10.1057/9781137311825.0009.

[57] N. Beaupere, U. Soupremanien, L. Zalewski, Nucleation triggering methods in supercooled phase change materials (PCM), a review, Thermochim. Acta 670 (2018) 184–201, https://doi.org/10.1016/j.tca.2018.10.009.

[58] S. Furbo, J. Fan, E. Andersen, Z. Chen, B. Perers, Development of seasonal heat storage based on stable supercooling of a sodium acetate water mixture, Energy Procedia 30 (2012) 260–269, https://doi.org/10.1016/j.egypro.2012.11.031.

[59] S. Furbo, S. Svendsen, Report on heat storage in a solar heating system using salt hydrates. Report no. 70. http://www.byg.dtu.dk/-/media/Institutter/Byg/publikationer/lfv/lfv/lfv_070.ashx?la=da, 1977.

[60] S. Furbo, Heat storage with an incongruently melting salt hydrate as storage medium based on the extra water principle, in: Thermal Storage of Solar Energy, Springer, Amsterdam, The Netherlands, 1980, pp. 135–145.

[61] M. Dannemand, J.M. Schultz, J.B. Johansen, S. Furbo, Long term thermal energy storage with stable supercooled sodium acetate trihydrate, Appl. Therm. Eng. 91 (2015) 671–678, https://doi.org/10.1016/j.applthermaleng.2015.08.055.

[62] M. Dannemand, W. Kong, J.B. Johansen, S. Furbo, Laboratory test of a prototype heat storage module based on stable supercooling of sodium acetate trihydrate, Energy Procedia 91 (2015) 172–181, https://doi.org/10.1016/j.egypro.2016.06.186.

[63] M. Dannemand, J.B. Johansen, W. Kong, S. Furbo, Experimental investigations on cylindrical latent heat storage units with sodium acetate trihydrate composites utilizing supercooling, Appl. Energy 177 (2016) 591–601, https://doi.org/10.1016/j.apenergy.2016.05.144.

[64] M. Dannemand, J. Dragsted, J. Fan, J.B. Johansen, W. Kong, S. Furbo, Experimental investigations on prototype heat storage units utilizing stable supercooling of sodium acetate trihydrate mixtures, Appl. Energy 169 (2016) 72–80, https://doi.org/10.1016/j.apenergy.2016.02.038.

[65] M. Dannemand, Compact Seasonal PCM Heat Storage for Solar Heating Systems, PhD Thesis, DTU Civil Engineering, 2016.

[66] G. Englmair, C. Moser, S. Furbo, M. Dannemand, J. Fan, Design and functionality of a segmented heat-storage prototype utilizing stable supercooling of sodium acetate trihydrate in a solar heating system, Appl. Energy 221 (2018) 522–534, https://doi.org/10.1016/j.apenergy.2018.03.124.

[67] G. Englmair, Y. Jiang, M. Dannemand, C. Moser, H. Schranzhofer, S. Furbo, J. Fan, Crystallization by local cooling of supercooled sodium acetate trihydrate composites for long-term heat storage, Energy Build. 180 (2018) 159–171, https://doi.org/10.1016/j.enbuild.2018.09.035.

[68] G. Englmair, C. Moser, H. Schranzhofer, J. Fan, S. Furbo, A solar combi-system utilizing stable supercooling of sodium acetate trihydrate for heat storage: numerical performance investigation, Appl. Energy 242 (2019) 1108–1120, https://doi.org/10.1016/j.apenergy.2019.03.125.

[69] G. Englmair, W. Kong, J. Brinkø Berg, S. Furbo, J. Fan, Demonstration of a solar combi-system utilizing stable supercooling of sodium acetate trihydrate for heat storage, Appl. Therm. Eng. 166 (2020), 114647, https://doi.org/10.1016/j.applthermaleng.2019.114647.

[70] G. Englmair, S. Furbo, M. Dannemand, J. Fan, Experimental investigation of a tank-in-tank heat storage unit utilizing stable supercooling of sodium acetate trihydrate, Appl. Therm. Eng. 167 (2020), 114709, https://doi.org/10.1016/j.applthermaleng.2019.114709.

[71] L. Desgrosseilliers, Design and Evaluation of a Modular, Supercooling Phase Change Heat Storage Device for Indoor Heating, PhD Thesis, Dalhousie University, Halifax, Nova Scotia, 2016.

[72] N. Beaupere, U. Soupremanien, L. Zalewski, Influence of water addition on the latent heat degradation of sodium acetate trihydrate, Appl. Sci. 11 (2021) 1–17, https://doi.org/10.3390/app11020484.

[73] M.A. Rogerson, S.S.S. Cardoso, Solidification in heat packs: I. Nucleation rate, AICHE J. 49 (2003) 505–515, https://doi.org/10.1002/aic.690490220.

[74] K. Yu, Y. Liu, Y. Yang, Review on form-stable inorganic hydrated salt phase change materials: preparation, characterization and effect on the thermophysical properties, Appl. Energy 292 (2021), 116845, https://doi.org/10.1016/j.apenergy.2021.116845.

[75] Y. Cui, J. Stojakovic, H. Kijima, A.S. Myerson, Mechanism of contact-induced heterogeneous nucleation, Cryst. Growth Des. 16 (2016) 6131–6138, https://doi.org/10.1021/acs.cgd.6b01284.

[76] P.G. Vekilov, Crystal nucleation: nucleus in a droplet, Nat. Mater. 11 (2012) 838–840, https://doi.org/10.1038/nmat3441.

[77] Z. Ma, H. Bao, A.P. Roskilly, Study on solidification process of sodium acetate trihydrate for seasonal solar thermal energy storage, Sol. Energy Mater. Sol. Cells 172 (2017) 99–107, https://doi.org/10.1016/j.solmat.2017.07.024.

[78] J. Lizana, A. Perejón, P.E. Sanchez-Jimenez, L.A. Perez-Maqueda, Advanced parametrisation of phase change materials through kinetic approach, J. Energy Storage 44 (2021), https://doi.org/10.1016/j.est.2021.103441.

[79] W.F. Green, The "Melting-point" of hydrated sodium acetate: solubility curves, J. Phys. Chem. 12 (1908) 655–660, https://doi.org/10.1021/j150099a002.

[80] N.V. Sidgwick, J.A.H.R. Gentle, in: The Solubilities of the Alkali Formates and Acetates in Water 1214, 1922, pp. 1837–1843.

[81] W.K.R. Watson, Heat Transfer System Employing Supercooled Fluids. U.S. Patent No 3952519, U.S. Patent No 3952519, 1976.

[82] T. Wada, Studies on Sodium Acetate Trihydrate for Latent Heat Storage, Osaka University, 1985.

[83] M. Faucheux, G. Muller, M. Havet, A. LeBail, Influence of surface roughness on the supercooling degree: case of selected water/ethanol solutions frozen on aluminium surfaces, Int. J. Refrig. 29 (2006) 1218–1224, https://doi.org/10.1016/j.ijrefrig.2006.01.002.

[84] S. Peng, Y. Hu, J. Huang, M. Song, Surface free energy analysis for stable supercooling of sodium thiosulfate pentahydrate with microcosmic-visualized methods, Sol. Energy Mater. Sol. Cells 208 (2020), 110390, https://doi.org/10.1016/j.solmat.2019.110390.

[85] S.K. Sharma, C.K. Jotshi, S. Kumar, Thermal stability of sodium salt hydrates for solar energy storage applications, Sol. Energy 45 (1990) 177–181, https://doi.org/10.1016/0038-092X(90)90051-D.

[86] X. Jin, S. Zhang, M.A. Medina, X. Zhang, Experimental study of the cooling process of partially-melted sodium acetate trihydrate, Energy Build. 76 (2014) 654–660, https://doi.org/10.1016/j.enbuild.2014.02.059.

[87] T.X. Li, J.X. Xu, D.L. Wu, F. He, R.Z. Wang, High energy-density and power-density thermal storage prototype with hydrated salt for hot water and space heating, Appl. Energy 248 (2019) 406–414, https://doi.org/10.1016/j.apenergy.2019.04.114.

[88] T. Xu, S.N. Gunasekara, J.N. Chiu, B. Palm, S. Sawalha, Thermal behavior of a sodium acetate trihydrate-based PCM: T-history and full-scale tests, Appl. Energy 261 (2020), 114432, https://doi.org/10.1016/j.apenergy.2019.114432.

[89] K. Sakurai, K. Sano, Mechanism of electrical nucleation in a latent heat storage device with supercooled aqueous solution of sodium acetate trihydrate, J. Cryst. Growth 516 (2019) 21–33, https://doi.org/10.1016/j.jcrysgro.2019.03.018.

[90] M.A. Rogerson, S.S.S. Cardoso, Solidification in heat packs: III. Metallic trigger, AICHE J. 49 (2003) 522–529, https://doi.org/10.1002/aic.690490222.

[91] G.L. Hogan, Device for Accumulating, Retaining and Discharguing Heat, U.S. Patent No 2289425, 1942.

[92] C.D. Snelling, Method and Means for Controllaby Releasing Heat From Supercooled Liquids, U.S. Patent No 3093308, 1963.

[93] D.E. Walters, O. Therm, Trigger to Activate Supercooled Aqueous Salt Solution for Use in a Heat Pack, U.S. Patent No 5662096, 1995.

[94] M.A. Rogerson, S.S.S. Cardoso, Solidification in heat packs: II. Role of cavitation, AICHE J. 49 (2003) 516–521, https://doi.org/10.1002/aic.690490221.

[95] E. Günther, H. Mehling, M. Werner, Melting and nucleation temperatures of three salt hydrate phase change materials under static pressures up to 800 MPa, J. Phys. D. Appl. Phys. 40 (2007) 4636–4641, https://doi.org/10.1088/0022-3727/40/15/042.

[96] G.I. Kapralis, J.E. Kapralis, J. Lowther, Imperforate Groove Trigger, U.S. Patent No 4899727, 1990.

[97] B. Sandnes, The physics and the chemistry of the heat pad, Am. J. Phys. 76 (2008) 546–550, https://doi.org/10.1119/1.2830533.

[98] D.K. Benson, P.F. Barret, Method and Apparatus for Nucleating the Crystallization of Undercooled Materials, U.S. Patent No 4860729, 1989.

[99] H. Mehling, L.F. Cabeza, Solid-liquid phase change materials, in: Heat and Cold Storage with PCM. An up to Date Introduction Into Basics and Applications, Springer, 2008, pp. 11–55.

[100] M.L. Smith, Trigger Device for Heat Pack, U.S. Patent No 4829980, 1989.

[101] M. Walters, Trigger to Activate Supercooled Aqueous Salt Solution for Use in a Heat Pack, U.S. Patent No 6878157, 2005.

[102] C.F. Manker, Activator for Initiating Reaction in a Heat Pack and Method for Making Same, U.S. Patent 4872442, 1989.

[103] S.P. Angelillo, R.H. Birdsey, Activator for Initiating Crystallization of a Supersaturated Solution, U.S. Patent No 5736110, 1989.

[104] T. Ohachi, M. Hamanaka, H. Konda, S. Hayashi, I. Taniguchi, T. Hashimoto, Y. Kotani, Electrical nucleation and growth of NaCH3COO·3H2O, J. Cryst. Growth 99 (1990) 72–76, https://doi.org/10.1016/0022-0248(90)90486-5.

[105] Y. Yoshii, M. Kuraoka, K. Sengoku, T. Ohachi, Induction time and three-electrode current vs. voltage characteristics for electrical nucleation of concentrated solutions of sodium acetate trihydrate, J. Cryst. Growth 237 (2000) 414–418, https://doi.org/10.19009/jjacg.27.1_65.

[106] T. Munakata, S. Nagata, Electrical initiation of solidification and preservation of supercooled state for sodium acetate trihydrate, in: 14th International Heat Transfer Conference, IHTC 14, 2010, pp. 383–388, https://doi.org/10.1115/IHTC14-22148.

[107] K. Seo, S. Suzuki, T. Kinoshita, I. Hirasawa, Effect of ultrasonic irradiation on the crystallization of sodium acetate trihydrate utilized as heat storage material, Chem. Eng. Technol. 35 (2012) 1013–1016, https://doi.org/10.1002/ceat.201100680.

[108] B.J.W. Mullin, K.D. Raven, Influence of mechanical agitation on the nucleation of some aqueous salt solutions, Nature 195 (1962) 35–38.

[109] P.D. Bloore, J.S.M. Botterill, Nucleation in agitated solutions, Nature 190 (1961) 251.

[110] R. Tamme, Behaviour of sodium acetate trihydrate in a dynamic latent heat storage system, in: AIAA 19th Thermophysics Conference, Colorado, 1984, https://doi.org/10.2514/6.1984-1740.

[111] N. Araki, M. Futamura, A. Makino, H. Shibata, Measurements of thermophysical properties of sodium acetate hydrate, Int. J. Thermophys. 16 (1995) 1455–1466, https://doi.org/10.1007/BF02083553.

[112] B. Zalba, L.F. Cabeza, H. Mehling, J.M. Marín, Review on thermal energy storage with phase change: materials, heat transfer analysis and applications, Appl. Therm. Eng. 23 (2003) 251–283, https://doi.org/10.1016/S1359-4311(02)00192-8.